



**HAL**  
open science

# On the use of drilling rotations for DIC-based identification of interface parameters in adhesive structural joints

Nunziante Valoroso

► **To cite this version:**

Nunziante Valoroso. On the use of drilling rotations for DIC-based identification of interface parameters in adhesive structural joints. 10e colloque national en calcul des structures, May 2011, Giens, France. pp.Clé USB. hal-00592699

**HAL Id: hal-00592699**

**<https://hal.science/hal-00592699>**

Submitted on 3 May 2011

**HAL** is a multi-disciplinary open access archive for the deposit and dissemination of scientific research documents, whether they are published or not. The documents may come from teaching and research institutions in France or abroad, or from public or private research centers.

L'archive ouverte pluridisciplinaire **HAL**, est destinée au dépôt et à la diffusion de documents scientifiques de niveau recherche, publiés ou non, émanant des établissements d'enseignement et de recherche français ou étrangers, des laboratoires publics ou privés.

# On the use of drilling rotations for DIC-based identification of interface parameters in adhesive structural joints

N. Valoroso

*Dipartimento per le Tecnologie, Università di Napoli Parthenope, Italy, nunziante.valoroso@uniparthenope.it*

**Abstract** — The problem of parameter identification via inverse analysis based on full-field kinematic data obtained via Digital Image Correlation (DIC) is discussed with special attention on resolving the surface motion of adhesive joints. The response up to failure of a DCB-like structure is simulated using either classical continuum and interface elements or membrane elements with drilling dofs and interface elements with drilling rotations along the bondline. Identification results are presented that show the differences between two such cases in terms of performances and parameter estimates.

**Keywords** — Adhesive joints, cohesive-zone models, identification, digital image correlation.

## 1 Introduction

In recent years adhesive bonding technologies have become widespread and almost commonplace in industry. Whether it be electronic components [1] or furniture, food packaging materials [2] or floor coverings, shoes or high-tech solutions [3], there is almost no product on the market today that is produced without adhesives. This virtually unlimited range of applications calls for an intensive research work in order to fully exploit the potential of adhesive joints.

As for most structural components consisting of the assembly of individual elements, failure of adhesive joints due to damage growth at bonded interfaces, leading to fracture development by sliding and separation, is one of the most important failure modes and for its simulation the cohesive zone concept initially proposed by Barenblatt [4] has become increasingly popular in the last decades. One of the reasons of its success is probably the flexibility of the cohesive approach to fracture, which provides an effective phenomenological description of the complex microscopic processes leading to the progressive decay of cohesive forces and the formation of traction-free surfaces.

For situations where interface positions are a priori known, cohesive models are used in conjunction with zero-thickness interface elements. These have to adequately resolve the process zone and be compatible with the surrounding continuum elements in order to obtain meaningful answers. Moreover, the availability of trustworthy estimates of material parameters that characterize the traction-relative displacement relationship and the general coherence between the data reduction schemes and the FE model in which the cohesive law is used are not secondary aspects, since the assumptions made for computing the material parameters from experiments have a direct impact on the results of computations.

In this study the fundamental problem of parameter identification via inverse analysis based on full-field kinematic data obtained via Digital Image Correlation (DIC) is discussed with special attention on resolving the surface motion of adhesive joints up to failure. This is not an easy task since computational failure analysis would require elements that are highly flexible and accurate, and with reduced sensitivity to mesh distortion, whilst for identification purposes elements with low number of nodes are quite desirable since they result in low connectivity of the structural stiffness matrix and reduced computational cost. Obviously, finding the optimal trade-off between accuracy and computational cost is critical.

The evaluation of mode-I parameters governing the damage mechanics-based formulation developed in [5] is addressed as the solution of a nonlinear programming problem. A least-squares norm is used as objective function that quantifies the distance between experimental data and the analogous quantities computed via finite elements as a function of the unknown parameters. The data set concern the deformation process of of a suitable region of interest extracted from the tested Double Cantilever Beam (DCB) specimen [6].

For the DCB problem at hand we suggest to simulate the response up to failure using interface elements with drilling rotations located along the bondline [7]. The interest of such elements is motivated by the fact that they can be coupled with membrane/shell elements with in-plane rotations, which are well-known to exhibit excellent accuracy and convergence features both for regular and distorted meshes, see e.g. [8]. The interface elements with drilling dofs have been implemented in a customized version of the finite element code FEAP [9] along with a suitable procedure for the computation of gradients of displacements and forces with respect to the material parameters, i.e. parameter sensitivities. These are indeed a key ingredient for identification purposes since, on one hand, they may allow to determine the location of measurements with the highest information content during experiments and, on the other side, can also provide the search direction in a gradient-based minimization algorithm.

The outline of the paper is as follows. In section 2 the cohesive model is briefly introduced; the interface element formulation is then recalled in section 3. The DCB test and the inverse identification problem are discussed in section 4; the results of identification based on truly experimental results in terms of full-field displacements data obtained via DIC are finally presented in section 5.

## 2 Cohesive damage model

The formulation of a cohesive-like model basically requires the definition of a relationship between interface tractions and displacement discontinuities and the introduction of a criterion for damage to grow and the process zone to move. In particular, we recall in the following the model proposed by Valoroso and Champaney [5] and consider the simplest two-parameter version for the mode I case, that is governed by the following equations :

$$\begin{aligned}
 t &= (1 - D)k\langle[[u]]\rangle_+ + k^-\langle[[u]]\rangle_- \\
 Y &= \frac{1}{2}k\langle[[u]]\rangle_+^2 \\
 \phi &= Y - Y^* \leq 0 \\
 \dot{Y}^* &= \dot{D} \frac{\partial F}{\partial D} \\
 \phi &\leq 0; \quad \dot{D} \geq 0; \quad \dot{D} \phi = 0
 \end{aligned} \tag{1}$$

where  $t$  and  $Y$  respectively denote the interface traction and the damage-driving force,  $D \in [0, 1]$  is the scalar damage variable,  $[[u]]$  is the displacement jump in the direction normal to the interface while  $k$  and  $k^-$  are the undamaged interface stiffnesses in tension and compression, respectively. The impenetrability constraint is introduced in penalty form via the stiffness coefficient  $k^-$  and by distinguishing between the positive and negative part of the displacement jump.

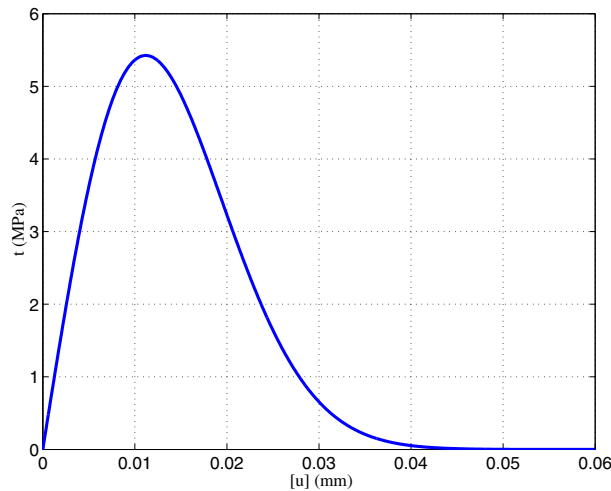


Figure 1 – Cohesive relationship to be identified, (see also [5])

The critical damage-driving force  $Y^*$  represents a non-decreasing energy threshold whose value is determined by a monotonically increasing positive function  $F$  given as :

$$Y^* = \begin{cases} \int_0^t \dot{Y}^* dt = F(D) & \text{if } D \in [0, 1[ \\ \max_{\tau \in [0, T]} Y(\tau) & \text{if } D = 1 \end{cases} \quad (2)$$

Typical forms of  $F$  are that of power laws or exponential functions, and their explicit expressions are constructed in a way to ensure that the energy dissipated in the formation of a new unit traction-free surface equals the critical strain energy release rate  $G_c$ . In particular, the two-parameter version of the exponential traction-separation relationship, see also Figure 1, is obtained using :

$$F(D) = -G_c \log(1 - D) \quad (3)$$

We recall that in the above model the computation of the damage state, is completely explicit ; in particular, for damage loading ( $\dot{D} > 0$ ) at each time  $\tau$  the damage variable is computed as :

$$D(\tau) = \min \left( 1, \max_{(\sigma \leq \tau)} \{F^{-1}(Y^*(\sigma))\} \right) \quad (4)$$

see also [5] for a detailed account.

In the following the vector collecting the two material parameters to be identified will be denoted as :

$$x = \begin{bmatrix} k \\ G_c \end{bmatrix} \quad (5)$$

### 3 Interface element formulation

A consistent variational framework for problems including in-plane rotational degrees of freedom has been presented by Hughes and Brezzi in [11]. In particular, in their formulation the stress tensor is not a priori assumed to be symmetric, whereby the role it plays in the theory is complementary to that of the (infinitesimal) rotation field.

The stiffness matrix of the drilling interface element can be obtained starting from the following degenerated Hughes-Brezzi functional [7] :

$$\Pi_\gamma(\mathbf{u}, \varphi, \boldsymbol{\tau}) = \frac{1}{2} \int_\Omega \mathbf{D}[[u]] \cdot [[u]] d\Omega + \int_\Omega \boldsymbol{\tau} \cdot (\mathbf{u}' - \varphi) d\Omega - \frac{1}{2} \gamma^{-1} \int_\Omega \boldsymbol{\tau}^2 d\Omega - \int_\Omega \mathbf{f} \cdot \mathbf{u} d\Omega \quad (6)$$

where  $\mathbf{u}$  is the displacement vector,  $\varphi$  is the drilling rotation,  $\boldsymbol{\tau}$  is a Lagrange multiplier that plays the same role of the skew-symmetric part of the stress in the continuum membrane element [10] and  $\gamma$  is a regularizing parameter to be chosen in accordance with the ellipticity condition.

Introducing the standard linear continuous finite element interpolations for displacements and rotations and adding quadratic modes for linking displacements to rotations, the discrete equations obtained by taking the variations of the above functional can be written in matrix form as [7] :

$$\begin{bmatrix} \mathbf{K}_u^e & \mathbf{g}^e \\ \mathbf{g}^{e,T} & -\frac{\Omega^e}{\gamma} \end{bmatrix} \begin{bmatrix} \mathbf{u}^I \\ \boldsymbol{\tau}^I \end{bmatrix} = \begin{bmatrix} \mathbf{f} \\ 0 \end{bmatrix} \quad (7)$$

The variable  $\boldsymbol{\tau}$  is in general assumed element-wise discontinuous, so that it can be eliminated using static condensation; hence, the stiffness matrix to be assembled at the global level is :

$$\mathbf{K}^e = \mathbf{K}_u^e + \frac{\gamma}{\Omega^e} (\mathbf{g}^e \otimes \mathbf{g}^e) \quad (8)$$

The individual terms of the stiffness matrix are evaluated using a three-point quadrature scheme. as shown in [7], either Newton-Cotes or Gauss quadrature yield the same identical result.

## 4 The DCB test and the identification problem

The Double Cantilever Beam is the standard test for obtaining the mode-I fracture toughness  $G_c$  of adhesives. Different procedures exist for performing the experiment and for data reduction ; in particular, corrected beam theories and compliance calibration methods are the most popular ones. However, apart from requiring the knowledge of the crack length evolution during the test, the mentioned data reduction schemes can exhibit possible incoherencies with the numerical model to be used for computations. For this reason, in the author's opinion the use of a Finite Element model to compute the material parameters should be preferred.

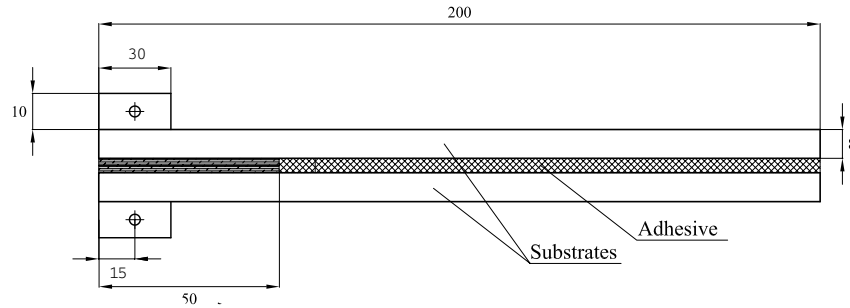


Figure 2 – DCB test specimen.

The geometry of the test considered is shown in Figure 2. The response of the DCB during the debonding tests is simulated using the interface model discussed in Section 4. This is taken as the constitutive law for interface elements, which have been implemented as a part of a customized version of the FE code FEAP [9]. In the numerical simulations the right-end of the structure (intact part) is free whilst on the left side two supports are prescribed and an increasing vertical displacements is imposed at the end of the upper arm. The experimental raw load-deflection curve is shown in Figure 3 in terms of reaction force  $P$  versus the relative displacement  $\delta$ .

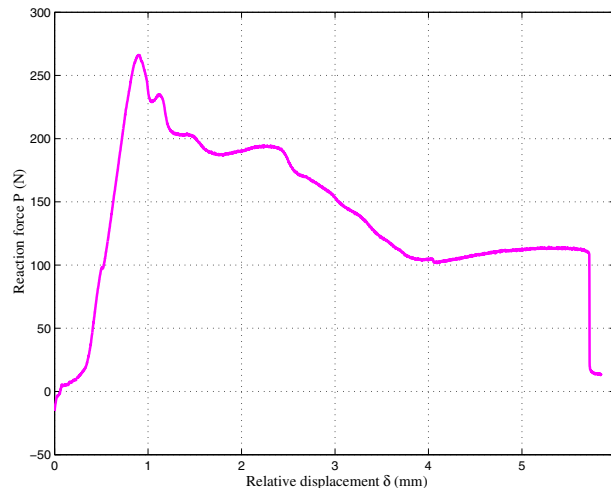


Figure 3 – DCB test. Experimental load-deflection curve.

The present study aims to effective identification of the material parameters of the interface model presented in section 2 via inverse analysis using as data set kinematic full-field data obtained from a DIC procedure [12, 13]. In a deterministic framework, the optimal material parameters  $\hat{x}$  can be obtained as the solution of a nonlinear programming problem where a suitable cost function is minimized. Such a function can be conveniently defined to represent, at all considered instants, the distance between *measured* quantities, i.e. displacements inside the monitored sub-domain, and those *computed* via the mathematical model as a function of the unknown parameters  $x$ .

The kinematic data set of the identification process (the *measured* kinematic quantities) is constituted by a time-space sampling of suitable displacements. In particular, it consists of a collection of  $n_u$ -dimensional vectors  $u_i^{meas}$  each referring to a particular instant  $t_i$ ,  $i = 1, \dots, n_t$ , of the loading process. The values of the same displacements that are instead *computed* via the FE model will be denoted as  $u_i^{comp}$ . With this notation in hand the identification problem is set as follows :

$$\hat{x} = \arg \min_{x \in \mathcal{S}} \omega(x) \quad (9)$$

for the cost function :

$$\omega(x) = \sum_{i=1}^{n_t} \left\{ \left\| u_i^{meas} - u_i^{comp}(x) \right\|_{\mathbf{W}_u^{-1}}^2 \right\} \quad (10)$$

$\mathcal{S}$  being is the constraint set, that in the present case is defined as the set of  $x$  that are component-wise positive :

$$\mathcal{S} = \{x \in \mathfrak{R} \mid x_j > 0, j = 1, 2\} \quad (11)$$

In the previous equation  $\mathbf{W}_u^{-1}$  denotes a weighting operator that scales the terms entering the definition of the residual in order to render them all of the same magnitude.

The minimization of the objective function (10) is performed through either using the Simplex method and/or a gradient-based descent algorithm available in the Matlab package [14], for which an interface has been developed to communicate with the FE code.

## 5 Results and discussion

Symmetric double cantilever beam (DCB) specimens were made using two 8 mm thick, 200.0 mm wide and 20.0 mm deep Al 2024 T351 aluminum coupons, bonded with a layer of acrylic adhesive and separated by an initial crack of length  $a = 50$  mm that is used as the starting defect. The tested DCB assembly was connected to the testing device using two 30mm-long by 10mm-thick fixtures after having coated the surface with sprayed black and white paints to create the random texture necessary for measuring kinematic fields measurement using DIC.

The experiment was monitored within a ROI of about  $70 \times 10 \text{mm}^2$  using a digital camera. The displacement field has been estimated using a correlation code relying upon a FE discretization that uses bilinear shape functions [13]; the element size in the FE mesh used for image correlation (typically of the order of some micrometers) being too small to be used for identification purposes, a suitable interpolation has been adopted in order to map the measured displacements onto the FE mesh to be used for identification.

Figure 4 shows at two different instants the kinematic measurements provided by DIC mapped onto a FE mesh that uses a discretization of  $1 \times 1 \text{mm}^2$  continuum elements. In the following are analyzed the results of identification exercises based on such data.

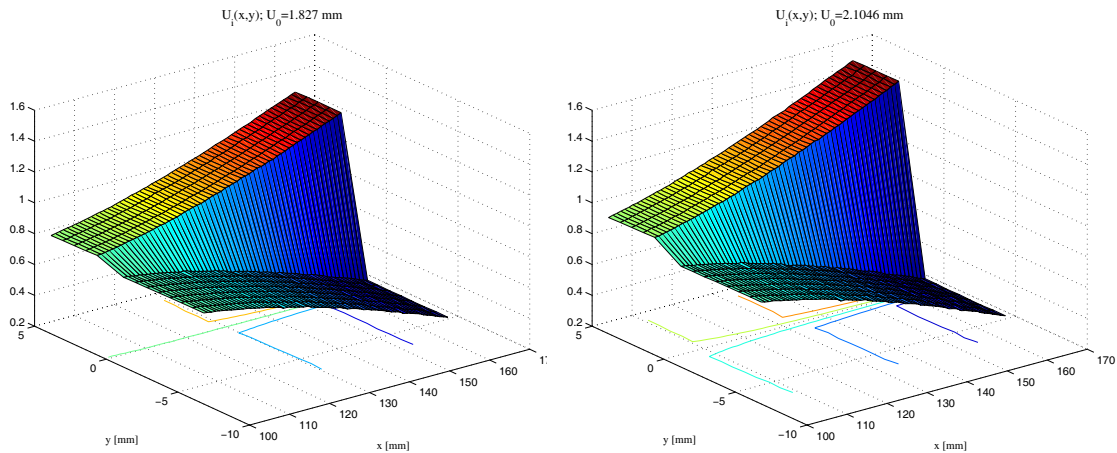


Figure 4 – DCB test. Interpolated displacement field computed via DIC at two different instants.

Computations are first carried out using a FE mesh of 4400 Enhanced Assumed Strain quadrilaterals and 150 interface elements. The result of identification is the vector :

$$x_1 = \begin{bmatrix} k \\ G_c \end{bmatrix} = \begin{bmatrix} 2583.875 N/mm^3 \\ 0.198390 N/mm \end{bmatrix} \quad (12)$$

Figure 5 shows the surface plot of the cost function of this series of identification exercises for a quite wide range of material parameters. The shape of the surface confirms what has been already noted in [6], i.e. that a good estimation of the fracture energy  $G_c$  is likely to be obtained in almost all cases, while a good estimate of the interface stiffness is more difficult.

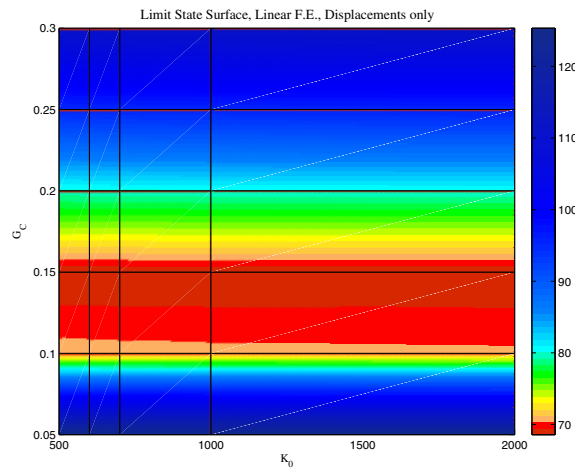


Figure 5 – Cost function surface. Classical continuum and interface elements

In the second series of computations use is made of a FE mesh consisting of 704 membrane elements 60 interface elements, both having drilling degrees of freedom. The result of identification is :

$$x_2 = \begin{bmatrix} k \\ G_c \end{bmatrix} = \begin{bmatrix} 5697.7076 N/mm^3 \\ 0.177167 N/mm \end{bmatrix} \quad (13)$$

Figure 6 shows the surface plot of the cost function of this series of identification exercises. Though the shape of the surface remains the same as before, the convergence path takes place almost for a constant value of the interface stiffness. However, the good performances of plane elements with drilling dofs for this problem are evident since the solution (13) is obtained for a much coarser mesh.

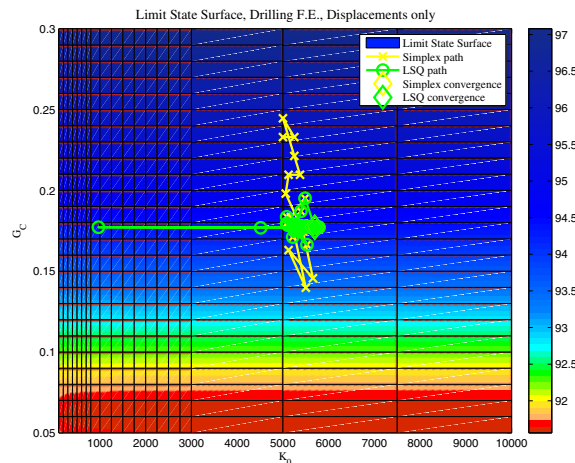


Figure 6 – Cost function surface. Continuum and interface elements with drilling dofs

In the third series of computations we tried to enrich the information content of the available measures by using an information about the rotation field that can be obtained from the available measurements of the displacement field. In particular, the drilling rotations computed using the interpolated nodal displacements on the adopted FE mesh and a finite difference scheme. The result is shown in Figure 7 in terms of additional data (the infinitesimal rotation field) and in Figure 8 in terms of cost function and convergence path of the minimization algorithms.

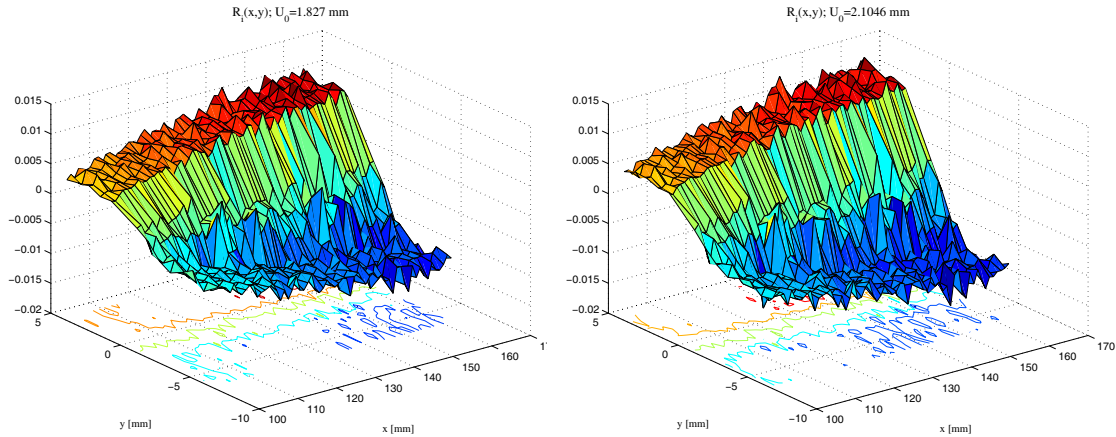


Figure 7 – DCB test. Rotation field computed using interpolated displacements obtained from mapping of DIC displacements.

In this case it is clearly seen that during the identification process the sequence generated by the minimization algorithms lies mostly along the steepest descent path. However, the solution vector

$$x_3 = \begin{bmatrix} k \\ G_c \end{bmatrix} = \begin{bmatrix} 5915.228 N/mm^3 \\ 0,036100 N/mm \end{bmatrix} \quad (14)$$

seems to be not very reliable since since the value of  $G_c$  is too close to the physical limit value 0.00.

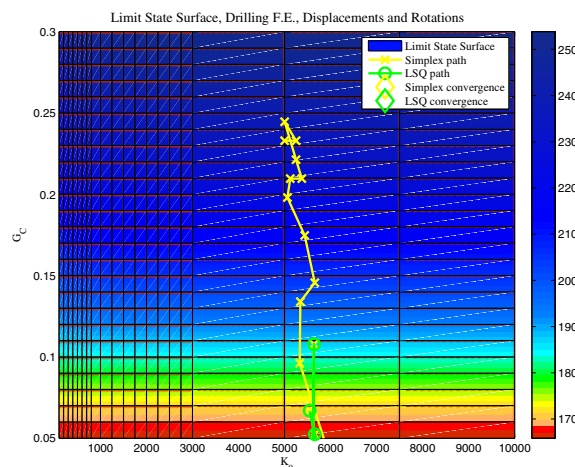


Figure 8 – Cost function surface. Continuum and interface elements with drilling dofs. Rotations included in data set

The reason of this apparent contradiction is probably the fact that in this case the quality of used data (i.e. their information content) is not of the same for displacements and rotations, whereby adding rotations into the data set has the effect of producing noise rather than improving precision. Improvements in the estimation of material parameters can however be achieved by properly using the results of the sensitivity analysis. The sensitivity information can indeed be very helpful in the development of

inverse analysis procedures since it can be taken as the basis of a selection criterion for the choice of the measurable quantities with the highest information content to be included in the cost function.

## Acknowledgements

This work has been carried out as part of the project *Analysis of structural adhesive joints. Modelling and experimental testing via DIC* within the MiSE-ICE-CRUI 2008 research program. The financial support of the Italian Ministry of Economic Development (MISE) and the Italian Institute for Foreign Trade (ICE) are gratefully acknowledged.

## References

- [1] Li, Y., Wong, C.P., 2006. Recent advances of conductive adhesives as a lead-free alternative in electronic packaging : Materials, processing, reliability and applications, *Materials Science and Engineering : R : Reports* 51(1-3), 1–35.
- [2] Choia, W.Y., Leeb, C.M., Parka, H.J., 2006. Development of biodegradable hot-melt adhesive based on poly-e-caprolactone and soy protein isolate for food packaging system, *LWT - Food Science and Technology* 39(6), 591–597.
- [3] Savage, G., 2006. Failure prevention in bonded joints on primary load bearing structures, *Engineering Failure Analysis* 14(2), 321–348.
- [4] Barenblatt, G.I., 1962. The mathematical theory of equilibrium cracks in brittle fracture, *Advances in Applied Mechanics* 7, 55–129.
- [5] Valoroso, N., Champaney, L., 2006 A damage-mechanics-based approach for modelling decohesion in adhesively bonded assemblies. *Engineering Fracture Mechanics*, 73, 2774–2801.
- [6] Valoroso, N., Fedele, R., 2010. Characterization of a cohesive-zone model describing damage and decohesion at bonded interfaces. Sensitivity analysis and mode-I parameter identification. *International Journal of Solids and Structures* 47(13), 1666–1677.
- [7] Valoroso, N., 2011. A novel interface element with rotational dofs, *Submitted for publication*.
- [8] Hughes, T.J.R., Masud, A., Harari, I., 1995. Numerical assessment of some membrane elements with drilling degrees of freedom. *Computers & Structures* 55(2), 297–314.
- [9] Taylor, R.L., 2009. FEAP, User and Programmer Manuals, *University of California at Berkeley*, <http://www.ce.berkeley.edu/~rlt>.
- [10] A. Ibrahimbegovic, R.L. Taylor and E.L. Wilson, A robust quadrilateral membrane finite element with drilling degrees of freedom, *International Journal for Numerical Methods in Engineering*, 30 :445–457, 1990.
- [11] Hughes, T.J.R., Brezzi, F., Harari, I., 1989. On drilling degrees of freedom, *Computer Methods in Applied Mechanics and Engineering*, 72, 105–121.
- [12] Hild, F., Roux, S., 2006. Digital image correlation : from measurement to identification of elastic properties - a review. *Strain* 42, 69–80.
- [13] Besnard, G., Hild, F., Roux, S., 2006. Finite-element displacement fields analysis from digital images : application to Portevin-Le Chatelier bands. *Experimental Mechanics* 46, 789–803.
- [14] The MathWorks Inc., 2009. Matlab 7.8 - Optimization Toolbox 4.2 Manual.